

# Biogas upgrading from vinasse digesters: a comparison between an anoxic biotrickling filter and an algal-bacterial photobioreactor

**Short title:** Biogas upgrading in anoxic biofilters and algal-bacterial photobioreactors

**Raquel Lebrero<sup>1\*</sup>, Alma Toledo-Cervantes<sup>1</sup>, Raúl Muñoz<sup>1</sup>, Valéria del Nery<sup>2</sup>, Eugenio Foresti<sup>2</sup>**

<sup>1</sup>Department of Chemical Engineering and Environmental Technology, University of Valladolid, Dr. Mergelina, s/n, 47011, Valladolid, Spain. Tel. +34 983186424, Fax: 983423013.

<sup>2</sup> Department of Hydraulics and Sanitation, School of Engineering, University of São Paulo, Av. Trabalhador São-Carlense, 400, CEP 13566-590, São Carlos, SP, Brazil

\* Corresponding author: raquel.lebrero@iq.uva.es

## Abstract

### BACKGROUND

The performance of an anoxic biotrickling filter (BTF) and an algal-bacterial photobioreactor (PBR) for the upgrading of real biogas was comparatively evaluated.

### RESULTS

A H<sub>2</sub>S removal efficiency of ~100% was consistently recorded in both systems, with elimination capacities of up to 1200 g S-H<sub>2</sub>S m<sup>-3</sup> h<sup>-1</sup> at low empty bed residence times (EBRTs ranging from 30 to 146 s). Both bioreactors demonstrated a high robustness towards fluctuations in biogas composition and flowrate, maintaining nearly complete desulfurization despite the variations in sulfur load and EBRT. The BTF also showed an immediate recovery from a 15 days operational shut-down, and the ability to utilize the nutrients from nitrate-supplemented digestate during biogas desulfurization. In addition, the PBR supported an average CO<sub>2</sub> removal of 23.0 ± 11.8 % at EBRT of 37-146 s and a carbon fixation rate of 285 mg CO<sub>2</sub> L<sup>-1</sup> d<sup>-1</sup>.

### CONCLUSIONS

The potential of anoxic biotrickling filters and algal-bacterial photobioreactors as efficient and robust technologies for the desulfurization of real biogas was demonstrated. The CO<sub>2</sub> fixation capacity of microalgae contributed to an enhanced biogas purification.

**Keywords:** algal-bacterial symbiosis, anoxic biofiltration, biogas upgrading, biotrickling filter, photobioreactor

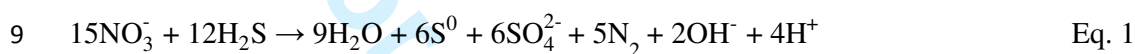
## 1 Introduction

2 The development of renewable energy sources has become a priority worldwide as a  
3 result of the steady rise in oil prices, the increasing dependence on fossil fuels, the  
4 gradual depletion of non-renewable energy sources and the increasing concern on global  
5 warming. Biogas from the anaerobic digestion of organic substrates constitutes a  
6 valuable bioenergy source that indeed contributes to the reduction of greenhouse gas  
7 (GHG) emissions.<sup>1-2</sup> Biogas production has steadily increased over the last years in the  
8 EU, with a total production of 13.4 Mtoe in 2013, which represents an increase of  
9 10.2% compared with the production in 2012.<sup>3</sup>

10 The type and content of organic substrate digested stoichiometrically determine the  
11 yield and composition of biogas, which usually contains CH<sub>4</sub> (50 to 75%), CO<sub>2</sub> (25 to  
12 50%), H<sub>2</sub>S (0 to 2%) and other gas pollutants such as siloxanes or NH<sub>3</sub> at trace level  
13 concentrations.<sup>1</sup> The presence of CO<sub>2</sub> and H<sub>2</sub>S in biogas hinders its direct use as a  
14 substitute of natural gas, biogas upgrading being essential in order to meet the required  
15 quality specifications for injection into natural gas grids or use as autogas. The high  
16 concentration of CO<sub>2</sub> increases biogas transportation costs and contributes to GHG  
17 emissions, besides reducing the specific biogas energy content. Likewise, a reduction in  
18 H<sub>2</sub>S content is crucial due to its odorous and toxic nature, and to the need to prevent  
19 corrosion and mechanical wear in biogas combustion systems. Indeed, H<sub>2</sub>S purification  
20 from biogas is sufficient for its direct combustion in the plant.

21 In this context, physicochemical technologies such as membrane separation, adsorption  
22 or scrubbing are capable of efficiently removing CO<sub>2</sub> and H<sub>2</sub>S from biogas, but at the  
23 expenses of prohibitive operating costs and high environmental impacts. On the other  
24 hand, biological biogas purification methods are capable of removing either CO<sub>2</sub>  
25 (conventional microalgae photobioreactors) or H<sub>2</sub>S (aerobic or denitrifying biotrickling

1 filtration) at significantly lower operating costs in a more environmentally friend way.<sup>2</sup>  
2 Aerobic H<sub>2</sub>S biotrickling filtration requires an external oxygen supply, which must be  
3 carefully controlled in order to avoid explosion risks and reduce the dilution of methane  
4 concentration in the purified biogas.<sup>4</sup> Autotrophic denitrification constitutes an  
5 alternative that overcomes these two operational problems based on sulfide oxidation  
6 via dissimilatory nitrate reduction (Eq. 1). In this technology, no mass transfer  
7 limitation of the electron acceptor occurs since nitrate is already dissolved in the  
8 tricking liquid media.<sup>2,5</sup>



10 Recent economic evaluations have demonstrated that the upgrading cost of one cubic  
11 meter of biogas amounts to 0.024 and 0.30 € m<sup>-3</sup> for FeCl<sub>3</sub> and chemical scrubbing,  
12 respectively, decreasing to 0.016 € m<sup>-3</sup> when anoxic biofiltration is applied.<sup>5,6</sup>  
13 However, this technology is only feasible as a pre-treatment for H<sub>2</sub>S removal from  
14 biogas.

15 In this context, the simultaneous removal of CO<sub>2</sub> and H<sub>2</sub>S by algal-bacterial symbiosis  
16 in photobioreactors represents a low-cost and environmentally-friendly alternative for  
17 an integral biogas upgrading. This technology is based on the fixation of CO<sub>2</sub> from  
18 biogas by microalgae using solar energy via photosynthesis, with the concomitant  
19 production of O<sub>2</sub>. Meanwhile, sulfur oxidizing bacteria will use this photosynthetically  
20 produced oxygen to oxidize the biogas H<sub>2</sub>S to sulfate according to Eq. 2.<sup>7,8</sup> This would  
21 avoid the operational problems of clogging often found in desulfurizing packed bed-  
22 biofilters due to elemental sulfur accumulation (Eq. 3).





6 2 In brief, algal-bacterial symbiosis and autotrophic denitrification have emerged in the  
7  
8 3 past years as promising platforms for biogas upgrading, but to the best of our  
9  
10 4 knowledge there are no studies comparing their performance during the upgrading of  
11  
12 5 real biogas emissions. This study aimed at comparatively evaluating the feasibility of an  
13  
14 6 algal-bacterial column photobioreactor and an anoxic biotrickling filter for the  
15  
16 7 upgrading of real biogas from two pilot scale Upflow Anaerobic Sludge Blanket  
17  
18 8 (UASB) reactors treating vinasse.  
19  
20  
21  
22  
23  
24

## 25 **Materials and Methods**

### 26 **Microorganisms and culture conditions**

27  
28  
29 12 Anaerobic sludge from a UASB reactor located in a poultry slaughterhouse (Dacar,  
30  
31 13 Tietê/SP, Brazil) was employed as the inoculum in the anoxic biotrickling filter (BTF).  
32  
33 14 The anaerobic sludge (200 mL) was acclimated for 45 days to the anoxic biodegradation  
34  
35 15 of sulfide in two bottles incubated at 35°C under continuous agitation and periodically  
36  
37 16 supplemented with Na<sub>2</sub>S (to a final concentration of 20 mg S<sup>-2</sup> L<sup>-1</sup>) and KNO<sub>3</sub> (to a  
38  
39 17 final concentration of 34 mg N-NO<sub>3</sub><sup>-</sup> L<sup>-1</sup>, ratio N/S = 1.7) under an argon headspace.  
40  
41 18 The Mineral salt medium (MSM) used for sludge acclimation and BTF operation was  
42  
43 19 composed of (mg L<sup>-1</sup>): NaHCO<sub>3</sub> (2000); KNO<sub>3</sub> (144); KH<sub>2</sub>PO<sub>4</sub> (36); NH<sub>4</sub>Cl (16);  
44  
45 20 MgCl<sub>2</sub>·6H<sub>2</sub>O (28) and CaCl<sub>2</sub>·2H<sub>2</sub>O (18). Trace elements were supplied by adding 2 mL  
46  
47 21 L<sup>-1</sup> of a stock solution containing (mg L<sup>-1</sup>): EDTA (500); ZnSO<sub>4</sub>·7H<sub>2</sub>O (40);  
48  
49 22 CaCl<sub>2</sub>·2H<sub>2</sub>O (70); MnCl<sub>2</sub> (30); (NH<sub>4</sub>)<sub>6</sub>Mo<sub>7</sub>O<sub>24</sub>·4H<sub>2</sub>O (10); CuSO<sub>4</sub>·H<sub>2</sub>O (20) and  
50  
51 23 CoCl<sub>2</sub>·6H<sub>2</sub>O (20).  
52  
53  
54  
55  
56  
57  
58  
59  
60

1  
2  
3 1 The photobioreactor (PBR) was inoculated with a mixture of aerobic sludge from an  
4  
5 2 activated sludge process (Volkswagen, São Carlos/SP, Brazil) and *Chlorella sp.*  
6  
7 3 (BIOTACE, Escola de Engenharia de São Carlos, São Paulo University). The aerobic  
8  
9 4 activated sludge (100 mL) was acclimated for 26 days to the aerobic biodegradation of  
10  
11 5 sulfide by periodical addition of Na<sub>2</sub>S to the cultivation broth (to a final concentration  
12  
13 6 of 20 mg S<sup>-2</sup> L<sup>-1</sup>) and renewal of the air headspace in order to ensure aerobic conditions.  
14  
15 7 *Chlorella sp.* was cultivated in 4 flasks of 200 mL for 9 days with atmospheric CO<sub>2</sub>  
16  
17 8 supply. The MSM used for aerobic sludge acclimation, *Chlorella sp.* cultivation and  
18  
19 9 PBR operation was composed of (mg L<sup>-1</sup>): NaNO<sub>3</sub> (85.0); CaCl<sub>2</sub>·2H<sub>2</sub>O (36.8);  
20  
21 10 MgSO<sub>4</sub>·7H<sub>2</sub>O (37.0); NaHCO<sub>3</sub> (12.6); Na<sub>2</sub>SiO<sub>3</sub>·9H<sub>2</sub>O (28.4) and K<sub>2</sub>HPO<sub>4</sub> (8.7); 1 mL  
22  
23 11 L<sup>-1</sup> of a trace elements solution and 1 mL L<sup>-1</sup> of a vitamins solution. The trace elements  
24  
25 12 stock solution was composed of (mg L<sup>-1</sup>): Na<sub>2</sub>EDTA·2H<sub>2</sub>O (4360); FeCl<sub>2</sub>·6H<sub>2</sub>O (3150);  
26  
27 13 CuSO<sub>4</sub>·5H<sub>2</sub>O (10); ZnSO<sub>4</sub>·7H<sub>2</sub>O (22); CoCl<sub>2</sub>·6H<sub>2</sub>O (10); MnCl<sub>4</sub>·4H<sub>2</sub>O (180);  
28  
29 14 Na<sub>2</sub>MoO<sub>4</sub>·2H<sub>2</sub>O (6) and H<sub>3</sub>BO<sub>3</sub> (1000); while the vitamins stock solution consisted of  
30  
31 15 (mg L<sup>-1</sup>): thiamine HCl (vitamin B1) (100); biotin (vitamin H) (0.5) and  
32  
33 16 cyanocobalamin (vitamin B12) (0.5).  
34  
35  
36  
37  
38  
39  
40  
41  
42

### 18 **Experimental set-up**

19 The biogas fed to both the BTF and the PBR was obtained from two pilot-scale UASB  
20  
21 20 digesters anaerobically treating vinasse. The PVC digesters had a working volume of 63  
22  
23 21 L (height = 2 m, diameter = 20 cm), a total volume of 126 L (4 m total height) and were  
24  
25 22 equipped with gas-solid separators according to Cavalcanti et al.<sup>9</sup> The digesters were  
26  
27 23 agitated via liquid recirculation to prevent biomass compaction. The vinasse was  
28  
29 24 collected in a sugarcane biorefinery and diluted to a final concentration of ~ 20 g COD  
30  
31  
32  
33  
34  
35  
36  
37  
38  
39  
40  
41  
42  
43  
44  
45  
46  
47  
48  
49  
50  
51  
52  
53  
54  
55  
56  
57  
58  
59  
60

1 L<sup>-1</sup>. The UASB reactors were operated at different organic loads and recirculation rates, resulting in varying biogas production rates and compositions.

The biotrickling filter consisted of a cylindrical PVC column with a total working volume of 2.5 L (height = 0.5 m, inner diameter = 0.08 m) (Figure 1A). The BTF was packed with 2 L of 1 cm<sup>3</sup> cubes of polyurethane foam inserted into plastic curls in order to provide the packing material with a higher structural stability. The BTF was operated at ambient temperature in a countercurrent flow configuration: the biogas from UASB 1 was fed from the bottom of the column, while MSM was continuously irrigated from the upper part of the bed. The trickling solution was conducted to a 1.75 L external tank (height = 0.25 m, inner diameter = 0.09 m) operated under continuous agitation and recycled at ~2 m h<sup>-1</sup> (diaphragm metering pump, Prominent, Germany).

The photobioreactor consisted of a transparent PVC column (total height = 0.9 m, inner diameter = 0.09 m) filled with 2 L of MSM and illuminated at ~230 μmol m<sup>-2</sup> s<sup>-1</sup> by 6 fluorescent lamps arranged in a circular configuration (Figure 1B). The algal-bacterial cultivation broth was continuously recycled from the top to the bottom of the PBR at 350 mL min<sup>-1</sup> (3.3 m h<sup>-1</sup>) in order to prevent biomass sedimentation. The biogas from UASB 2 was fed via a ceramic sparger from the bottom of the PBR, which was operated at ambient temperature.

## Bioreactors operation

The acclimated anaerobic sludge (200 ml with a total suspended solid (TSS) and volatile suspended solid (VSS) concentration of 3.9 ± 0.1 and 1.7 ± 0.0 g L<sup>-1</sup>, respectively) was mixed with the BTF packing material. After inoculation, the BTF was operated for 73 days with synthetic MSM. From day 74 onward, the effluent from the

1 anaerobic digester previously aerated for 24 hours and supplemented with  $\text{NO}_3^-$  (by  
2 means of  $\text{NaNO}_3$  addition to an initial concentration of  $3 \text{ g NO}_3^- \text{ L}^{-1}$ ) was used as a  
3 nutrient and electron donor source (simulating a partially nitrified digestate) in order to  
4 integrate biogas upgrading and wastewater treatment. For the first 47 days, 200 mL of  
5 MSM were daily exchanged, increasing the MSM (or digestate) exchange rate to 250  
6  $\text{mL day}^{-1}$  from day 48 onward in order to prevent sulfate build-up. The digestate was  
7 characterized by a COD concentration of  $1.82 \pm 0.5 \text{ g O}_2 \text{ L}^{-1}$ , a sulfate concentration of  
8  $139.6 \pm 38.5 \text{ mg L}^{-1}$ , an alkalinity of  $3553 \pm 494 \text{ mg L}^{-1}$  and a  $\text{pH} = 8.1 \pm 0.2$ . The pH of  
9 the tricking solution was manually adjusted to  $\sim 7$  by addition of  $\text{NaOH}$  (2 M) for an  
10 optimum growth of the denitrifying community. A shutdown period due to digester  
11 operational failure occurred from days 28 to 46. During the experimentation period, the  
12 biogas empty bed residence times (EBRTs) ranged from 30 to 100 s as a result of the  
13 variation on the biogas productivity of UASB 1.

14 The photobioreactor was inoculated with a mixture of acclimated aerobic sludge (200  
15 ml with a TSS of  $0.6 \text{ g L}^{-1}$  and a VSS concentration of  $0.3 \text{ g L}^{-1}$ , respectively) and  
16 *Chlorella sp.* (800 mL with a VSS concentration of  $0.2 \text{ g L}^{-1}$ ). The PBR was operated  
17 for 62 days at EBRTs ranging from 37 up to 146 s as a result of the variation on the  
18 biogas productivity of UASB 2. The pH was manually adjusted to  $\sim 7$  by  $\text{NaOH}$  (2 M)  
19 addition. Cultivation medium (250 mL) was daily replaced with fresh MSM in order to  
20 provide nutrients for microalgal growth and prevent sulfate accumulation.

21 The inlet and outlet biogas composition ( $\text{CH}_4$ ,  $\text{CO}_2$ ,  $\text{N}_2$  and  $\text{H}_2\text{S}$ ) from both bioreactors  
22 was daily analyzed in a GC-TCD. Liquid samples were also periodically withdrawn  
23 from both bioreactors for the determination of sulfide, sulfate, thiosulfate, nitrite and  
24 nitrate concentrations. The optical density from the liquid medium of the PBR was also  
25 analyzed. Finally, biomass samples from the inoculum, the digestate and the BTF

1 packed bed at three different heights at the end of the operation were collected and  
2 stored at  $-20\text{ }^{\circ}\text{C}$  in order to evaluate the evolution of the bacterial communities.

#### 4 **Analytical procedures**

5  $\text{CH}_4$ ,  $\text{CO}_2$ ,  $\text{N}_2$  and  $\text{H}_2\text{S}$  gas concentrations were analyzed in a Shimadzu GC-2014  
6 coupled with a thermal conductivity detector and equipped with a HP-PLOT/Q (30 m  $\times$   
7 0.54 mm  $\times$  40  $\mu\text{m}$ ) column. The injector and detector temperatures were set at 160 and  
8 170  $^{\circ}\text{C}$ , respectively. The oven temperature was initially maintained at 35  $^{\circ}\text{C}$  for 2 min,  
9 and increased at 60  $^{\circ}\text{C min}^{-1}$  up to 170  $^{\circ}\text{C}$ . Hydrogen was used as the carrier gas at 24  
10  $\text{mL min}^{-1}$ . Sulfide concentration in the liquid phase was determined by the colorimetric  
11 methylene blue method, while sulfate, thiosulfate, nitrite and nitrate concentrations were  
12 analyzed by HPLC-IC according to Standard Methods for the Examination of Water  
13 and Wastewater.<sup>10</sup> The culture absorbance was analyzed by spectrophotometry (Hach  
14 DR/4000V, US).

15 The polyacrylamide DGGE gels for the characterization of the bacterial communities  
16 were made with denaturing gradient ranging from 45 to 65% (where 100% denaturant  
17 contains 7 M urea and 40% (v/v) deionized formamide). The electrophoresis was run for  
18 16 h at 60  $^{\circ}\text{C}$  and 75 V. The gel was stained with ethidium bromide and imaging was  
19 performed using an Eagle Eye TM III (Stratagene) at a UV wavelength of 254 nm. Gel  
20 images were analyzed using Bionumerics Software Vers.2.5 (Applied Maths, Belgium).  
21 The similarity coefficients of the DGGE profiles were calculated using the Pearson  
22 correlation coefficients (densitometric curve-based) and clustered using UPGMA  
23 (Unweighted Pair Group Method with Arithmetic).



1

## 2 **Results and Discussion**

### 3 **Anoxic biotrickling filter**

4 The composition of the raw biogas fed to the anoxic BTF varied from 47 to 74% v/v for  
5 CH<sub>4</sub>, from 16 to 48% v/v for CO<sub>2</sub> and from 0.4 to 3.7% v/v for H<sub>2</sub>S, depending on the  
6 performance of UASB 1 (Figure 2A). From day 6 to 28, no H<sub>2</sub>S was detected in the  
7 upgraded biogas regardless of the fluctuations in the EBRT, which ranged from 30 up to  
8 100 s (Figure 2A). This removal efficiency (RE) > 99% was immediately restored after  
9 the resumption of biogas feeding following the 15-days shutdown period. Moreover, the  
10 substitution of the recycling synthetic MSM by NO<sub>3</sub><sup>-</sup>-supplemented effluent from the  
11 anaerobic digester did not result in a deterioration of the BTF performance, a complete  
12 H<sub>2</sub>S removal being maintained until the end of the operating period (Figure 2B). The  
13 desulfurization performance was not affected by the sulfur inlet load (IL), which varied  
14 from 187 to 1260 g S m<sup>-3</sup> h<sup>-1</sup> (Figure 3B). This demonstrated the robustness of the  
15 anoxic BTF under real operating conditions (with inherent variations in the composition  
16 and flow rate of the biogas). In this sense, both a sustained elimination capacity (EC) of  
17 677 ± 236 g S-H<sub>2</sub>S m<sup>-3</sup> h<sup>-1</sup> during steady state operation and a maximum EC of 1260 g  
18 S-H<sub>2</sub>S m<sup>-3</sup> h<sup>-1</sup> were found at a 100 % removal efficiency, even at the lowest EBRT of 30  
19 s, while previous studies observed a critical EBRTs of 90 s for a complete anoxic  
20 degradation of H<sub>2</sub>S in BTFs.<sup>2, 11</sup> On the contrary, no significant reductions in CH<sub>4</sub> or  
21 CO<sub>2</sub> concentrations were recorded despite the high H<sub>2</sub>S RE achieved, with average  
22 decreases in the outlet biogas concentrations of 1.7 ± 2.7 % for CH<sub>4</sub>, and 4.0 ± 5.2 % for  
23 CO<sub>2</sub> (Figure 2B). This absence of methane removal constitutes one of the main  
24 advantages of anoxic over aerobic desulfurization, where dilution of the upgraded

1  
2  
3 1 biogas as a result of O<sub>2</sub> and N<sub>2</sub> (when using air as a source of O<sub>2</sub>) addition is  
4  
5 2 unavoidable.<sup>2</sup>  
6  
7

8 3 In order to ensure that H<sub>2</sub>S was not only removed by physical absorption into the  
9  
10 4 trickling liquid but also biologically oxidized, sulfide and sulfate concentrations in the  
11  
12 5 liquid phase were periodically analyzed. Accumulation of S<sup>2-</sup> was only detected  
13  
14 6 immediately following the start-up and resumption of the BTF (Figure 3A). Hence, S<sup>2-</sup>  
15  
16 7 concentration reached 7.5 mg S<sup>2-</sup>L<sup>-1</sup> by day 9 and averaged 0.49 ± 0.28 mg S<sup>2-</sup>L<sup>-1</sup> from  
17  
18 8 days 11 to 28. Likewise, S<sup>2-</sup> concentration initially increased for two days following  
19  
20 9 biogas resumption up to a maximum concentration of 11.5 mg S<sup>2-</sup>L<sup>-1</sup> by day 47.  
21  
22 10 However, from day 50 onward, stable concentrations of S<sup>2-</sup> of 0.31 ± 0.30 mg S<sup>2-</sup>L<sup>-1</sup> in  
23  
24 11 the recycling medium were recorded despite supplementing the BTF with digester  
25  
26 12 effluent. Similarly, thiosulfate was not detected in the liquid phase during the entire  
27  
28 13 experimentation period. Therefore, the biological degradation of the H<sub>2</sub>S transferred  
29  
30 14 from the biogas was confirmed as sulfide was mainly oxidized to either sulfate or  
31  
32 15 elemental sulfur according to Eq. 1. In this sense, sulfate initially accumulated during  
33  
34 16 the first 28 days of operation reaching a maximum concentration of ~1.0 g S-SO<sub>4</sub><sup>2-</sup>L<sup>-1</sup>  
35  
36 17 by day 23 (Figure 3A). The MSM renewal rate was increased from 200 mL day<sup>-1</sup> to 250  
37  
38 18 mL day<sup>-1</sup> from day 46 onward in order to decrease the SO<sub>4</sub><sup>2-</sup> concentration in the  
39  
40 19 recycling media. This operational change resulted in maximum sulfate concentrations of  
41  
42 20 0.66 g SO<sub>4</sub><sup>2-</sup>L<sup>-1</sup> by day 55 and in a gradual decrease to stable values of 0.37 ± 0.03 g  
43  
44 21 SO<sub>4</sub><sup>2-</sup>L<sup>-1</sup> from days 62 to 73. The concentrations here recorded remained under the  
45  
46 22 inhibitory values reported in literature (e.g. critical S-SO<sub>4</sub><sup>2-</sup> concentration of 11 g L<sup>-1</sup> at  
47  
48 23 high sulfur ILs).<sup>5</sup>  
49  
50  
51  
52  
53  
54  
55  
56  
57  
58  
59  
60

1  
2  
3 1 A partial oxidation of  $S^{2-}$  to  $S^0$  has been widely reported in anoxic BTFs, the ratio  
4  
5 2 between the nitrate supplied ( $\text{mol N-NO}_3^-$ ) and the sulfide removed ( $\text{mol S-H}_2\text{S}$ )  
6  
7 3 determining the  $\text{S-SO}_4^{2-}/\text{S}^0$  ratio obtained.<sup>11, 12</sup> A sulfur mass balance was performed by  
8  
9 4 subtraction in order to estimate the amount of sulfur produced in the reactor.<sup>13</sup> In our  
10  
11 5 particular study, the molar N/S ratio fluctuated along the BTF operation from 0.4 to 1.3  
12  
13 6  $\text{mol mol}^{-1}$  as a result of the fluctuating  $\text{H}_2\text{S}$  ILs. These values were below the minimum  
14  
15 7 N/S ratio of  $1.6 \text{ mol mol}^{-1}$  required for complete  $\text{H}_2\text{S}$  oxidation to sulfate.<sup>14</sup> This was  
16  
17 8 confirmed by the  $\text{S-SO}_4^{2-}/\text{S}^0$  ratios estimated from a sulfur mass balance, which  
18  
19 9 fluctuated from 5% to 84%. Several authors have reported the feasibility to control the  
20  
21 10 oxidation products by modifying the N/S ratio during operation at a constant IL.<sup>15</sup>  
22  
23 11 However, no clear correlation between the N/S molar ratio and the sulfate selectivity  
24  
25 12 was observed in our particular system, despite the higher N/S molar ratios entailed  
26  
27 13 higher  $\text{S-SO}_4^{2-}/\text{S}^0$  values (e.g.  $1.1 \text{ mol mol}^{-1}$  resulted in 84%  $\text{SO}_4^{2-}$  conversion). These  
28  
29 14 results could be attributed to the rapidly changing conditions in the BTF and the  
30  
31 15 unstable nitrate and  $\text{H}_2\text{S}$  concentrations. Thus, a precise control of the sulfide oxidation  
32  
33 16 by programmed  $\text{NO}_3^-$  feeding might not be feasible under real operating conditions, as  
34  
35 17 previously stated by Fernández et al.,<sup>5</sup> due to the rapidly changing  $\text{H}_2\text{S}$  loads.

36  
37  
38  
39  
40  
41 18 Both the supply and concentration of nitrate must be carefully controlled as it acts as the  
42  
43 19 electron acceptor for sulfide-oxidizing bacteria. Nitrate initially accumulated in the  
44  
45 20 liquid media reaching a concentration of  $\sim 415 \text{ mg N-NO}_3^- \text{ L}^{-1}$  by day 26 (Figure 3A). In  
46  
47 21 order to avoid nitrate build-up in the liquid phase, the concentration of nitrate in the  
48  
49 22 fresh MSM was decreased after reactor resumption, resulting into roughly stable nitrate  
50  
51 23 concentrations of  $375 \pm 43 \text{ mg N-NO}_3^- \text{ L}^{-1}$  from day 61 onward. According to previous  
52  
53 24 studies, a minimum nitrate concentration of  $20 \text{ mg N-NO}_3^- \text{ L}^{-1}$  is required to maintain  
54  
55 25 maximum  $\text{H}_2\text{S}$  removals at an  $\text{IL} = 4.9 \text{ g S m}^{-3} \text{ h}^{-1}$ ,<sup>15</sup> thus no nitrate limitation was  
56  
57  
58  
59  
60

1  
2  
3 1 likely to occur during the experimental period. The recorded nitrate reduction rates,  
4  
5 2 which ranged from 0.01 to 0.1 g N-NO<sub>3</sub><sup>-</sup> L<sup>-1</sup> d<sup>-1</sup>, fluctuated concomitantly with the H<sub>2</sub>S  
6  
7 3 load (Figure 3B). These reduction rates were in accordance with previous denitrification  
8  
9 4 data in anoxic BTFs, although they were highly dependent on the nitrate concentration  
10  
11 5 and the H<sub>2</sub>S IL. <sup>5</sup>The rapid reduction of nitrate compared with that of nitrite resulted in  
12  
13 6 the accumulation of this latter intermediate product in the liquid media. Thus, N-NO<sub>2</sub><sup>-</sup>  
14  
15 7 concentration gradually increased to stable values of 96 ± 15 and 183 ± 41 mg N-NO<sub>2</sub><sup>-</sup>  
16  
17 8 L<sup>-1</sup> following the start-up and resumption of BTF operation, no inhibitory effect being  
18  
19 9 observed due to its accumulation. Previous studies operated at nitrite concentrations of  
20  
21 10 up to 300 mg N-NO<sub>2</sub><sup>-</sup> L<sup>-1</sup> reported no significant inhibition of the performance of the  
22  
23 11 anoxic biofiltration process. <sup>5,14</sup>

24  
25  
26  
27  
28 12 A typical liquid recycling velocity (U<sub>L</sub>) of 2 m h<sup>-1</sup> was set in the BTF. Despite prior  
29  
30 13 studies have reported clear effects of the U<sub>L</sub> on the H<sub>2</sub>S mass transfer from the gas to the  
31  
32 14 liquid phase (and therefore on H<sub>2</sub>S removal), the ILs prevailing during the complete  
33  
34 15 experimental period never resulted in mass transfer limitations. In this sense, minimum  
35  
36 16 trickling velocities of 4.6 and 15 m h<sup>-1</sup> are recommended when working at IL > 93 and  
37  
38 17 201 g S m<sup>-3</sup> h<sup>-1</sup>, respectively. <sup>2,5</sup> Moreover, previous studies addressing the influence of  
39  
40 18 U<sub>L</sub> and EBRT on the volumetric mass transfer coefficient (k<sub>L</sub>a) of methane in a BTF  
41  
42 19 demonstrated a low sensitivity of this parameter towards variations in the liquid  
43  
44 20 recycling velocity during operation at high EBRTs. <sup>16</sup>

45  
46  
47  
48  
49 21 Finally, the microbiological analysis showed an acclimation of the microbial  
50  
51 22 communities along the experimental period together with a decrease in bacterial  
52  
53 23 diversity (Figure 4), which could be confirmed by the low similarity between both the  
54  
55 24 inoculum and vinasse samples and the communities developed in the BTF. However,  
56  
57  
58  
59  
60

1  
2  
3 1 similar populations (>86% similarity) were established throughout the packed bed as  
4  
5 2 shown by the DGGE profile of R1, R2 and R3.  
6  
7  
8  
9

#### 10 4 **Photobioreactor**

11  
12  
13 5 Biogas from UASB 2 exhibited an average composition of  $73 \pm 4.9 \%$  for  $\text{CH}_4$ ,  $21.5 \pm$   
14  
15 6  $5.6 \%$  for  $\text{CO}_2$ ,  $5 \pm 2.5 \%$  for  $\text{N}_2$  and  $0.5 \pm 0.2 \%$  for  $\text{H}_2\text{S}$ . On the other hand, the biogas  
16  
17 7 flow rate ranged from  $0.8$  to  $3.3 \text{ L h}^{-1}$ , resulting in EBRTs from  $37$  up to  $146 \text{ s}$  (Figure  
18  
19 8 5A). Complete  $\text{H}_2\text{S}$  removal was recorded in the PBR regardless of the EBRT and the  
20  
21 9 IL, achieving maximum ECs of  $1052 \text{ g S-H}_2\text{S m}^{-3} \text{ h}^{-1}$  (Figure 5B). This sustained  $\text{H}_2\text{S}$   
22  
23 10 abatement despite the variations in biogas composition and flowrate confirmed the high  
24  
25 11 desulfurization robustness of the FBR. However, a varying  $\text{CO}_2$  removal was recorded  
26  
27 12 during the complete experimentation period. A  $\text{CO}_2$  fixation rate of  $285 \text{ mg-CO}_2 \text{ L}^{-1} \text{ d}^{-1}$   
28  
29 13 (assuming  $0.5 \text{ g C}$  per gram of biomass) was achieved based on the maximum biomass  
30  
31 14 productivity recorded during the first 25 days of experimentation. The carbon mass  
32  
33 15 balance showed that  $100\%$  of the  $\text{C-CO}_2$  removed in the PBR was recovered as  
34  
35 16 biomass. It was thus hypothesized that the low  $\text{CO}_2$  mass transfer recorded, likely  
36  
37 17 mediated by the low pH and to the low EBRT tested, might have limited microalgal  
38  
39 18 growth and hence  $\text{CO}_2$  removal from biogas. In this sense, the C-fixation rate resulted in  
40  
41 19 removal efficiencies in the PBR ranging from  $4.2$  to  $57.4 \%$ , with an average RE of  $23.0$   
42  
43 20  $\pm 11.8 \%$  (Figure 5B). In order to elucidate the limiting step during biogas in the PBR,  
44  
45 21 an experiment was performed by day 62 which consisted of increasing the pH of the  
46  
47 22 cultivation medium to  $8.1$  by NaOH addition and measuring the corresponding  $\text{CO}_2$   
48  
49 23 concentration in the gas phase (data not shown). The results showed that the enhanced  
50  
51 24  $\text{CO}_2$  concentration gradient between the bulk gas phase and the aqueous phase at a  
52  
53 25 higher pH supported  $\text{CO}_2$  removals of  $62\%$ . Thus, a better biogas upgrading  
54  
55  
56  
57  
58  
59  
60

1 performance in the PBR would be expected at higher operational pHs as a result of the  
2 enhanced CO<sub>2</sub> mass transfer and the herein confirmed subsequent CO<sub>2</sub> sequestration by  
3 microalgae.<sup>17</sup> At this point it should be highlighted that the pH in the PBR was  
4 maintained at 7 to allow for a fair performance comparison with the anoxic BTF.  
5 Finally, a negligible average methane removal of 5.7 ± 4.6 % was recorded in the PBR  
6 (Figure 5B). Moreover, no inhibition of the microalgal-bacterial activity at methane  
7 concentrations of up to 80 % was observed, as recently demonstrated by Wand and co-  
8 workers<sup>18</sup>. The maximum growth rate estimated (155 g L<sup>-1</sup> d<sup>-1</sup>) was comparable with  
9 previous reported values for *Chlorella* sp. MB-9 cultures (276 g L<sup>-1</sup> d<sup>-1</sup>) supplemented  
10 with artificial biogas with a composition of 80% of CH<sub>4</sub> and 20% of CO<sub>2</sub>.<sup>19</sup>

11 The initial increase in sulfate concentration in the cultivation medium up to ~400 mg S-  
12 SO<sub>4</sub><sup>-2</sup> L<sup>-1</sup> by day 24 and its subsequent stabilization at 409 ± 67 mg S-SO<sub>4</sub><sup>-2</sup> L<sup>-1</sup> showed  
13 that H<sub>2</sub>S was not only transferred from the biogas to the liquid phase, but also  
14 biologically oxidized according to Equation 2 (Figure 6). This result was further  
15 confirmed by the low S<sup>2-</sup> concentrations recorded, which remained constant throughout  
16 the experimental period at 1.0 ± 0.4 mg S<sup>2-</sup> L<sup>-1</sup> (Figure 6). In this context, the  
17 measurement of the dissolved O<sub>2</sub> concentration showed a roughly stable value of ~ 2.3  
18 mg L<sup>-1</sup> as a result of the balance between the photosynthetically O<sub>2</sub> produced and the O<sub>2</sub>  
19 consumed by bacteria for H<sub>2</sub>S oxidation. This guaranteed the almost complete oxidation  
20 to sulfate of the H<sub>2</sub>S transferred from the biogas.

21 Whereas several authors have previously investigated the CO<sub>2</sub> fixation capacity of  
22 *Chlorella* sp.,<sup>17-19</sup> the number of studies devoted to elucidate the potential of this  
23 microalga for biogas upgrading is still scarce. In this context, Mann et al.<sup>20</sup> successfully  
24 eliminated up to 97% of CO<sub>2</sub> and 100% of H<sub>2</sub>S from a synthetic biogas (41 % CO<sub>2</sub> and  
25 438 ppm<sub>v</sub> H<sub>2</sub>S) in a batch biogas upgrading experiment (gas residence time = duration

1  
2  
3 1 of the experiment) conducted in tubular photobioreactor. Nevertheless, the upgraded  
4  
5 2 biogas was contaminated with a high content of oxygen with the subsequent decrease in  
6  
7 3 methane content. Following this study, Bahr et al. and Serejo et al.<sup>7,21</sup> demonstrated the  
8  
9 4 potential of an alkaliphilic microalgal-bacterial consortium for the simultaneous  
10  
11 5 removal of H<sub>2</sub>S and CO<sub>2</sub> from biogas coupled with nutrient removal from centrates and  
12  
13 6 anaerobically digested vinasse, respectively. The pilot high-rate algal ponds  
14  
15 7 interconnected to external CO<sub>2</sub>-H<sub>2</sub>S absorption columns used in those studies supported  
16  
17 8 removals of 100 % from H<sub>2</sub>S and 40-80 % for CO<sub>2</sub>. However, these high CO<sub>2</sub> removals  
18  
19 9 were obtained at the expenses of an additional gas-liquid absorption stage operated at  
20  
21 10 significantly higher EBRTs (from 16 min up to 8.3 hours) than those tested in our study  
22  
23 11 (37 - 146 s). Moreover, the composition of the synthetic biogas used by Bahr et al. and  
24  
25 12 Serejo et al.<sup>7,21</sup> was constant and H<sub>2</sub>S concentration was <5000 ppm<sub>v</sub>, far below the  
26  
27 13 values reached by the UASB biogas treated in our system. Finally, it is important to  
28  
29 14 remark that, despite the CO<sub>2</sub> removal efficiencies here obtained were moderate, they  
30  
31 15 were comparable to those achieved under indoors microalgae cultivation, and higher  
32  
33 16 fixation rates, and therefore enhanced CO<sub>2</sub> removals from biogas, would be expected if  
34  
35 17 the PBR was operated outdoors.  
36  
37  
38  
39  
40  
41  
42

43  
44 19 In brief, the desulfurization performance achieved in both BTF and PBR was similar,  
45  
46 20 although slightly lower S<sup>2-</sup> concentrations were recorded in the liquid medium of the  
47  
48 21 BTF. Both systems exhibited a high robustness towards the variations in biogas flowrate  
49  
50 22 and composition typically found in real biogas from anaerobic digesters. Moreover, the  
51  
52 23 desulfurization capacity of the BTF was immediately recovered after a 15-days biogas  
53  
54 24 shutdown. Despite CO<sub>2</sub> removal in the PBR was limited by the mass transport of this  
55  
56 25 biogas pollutant to the aqueous phase, higher removals were recorded compared with  
57  
58  
59  
60

1  
2  
3 1 those of the BTF. This study confirmed the potential of the symbiosis between  
4  
5 2 microalgae and bacteria as a technological platform for the simultaneous removal of  
6  
7 3 CO<sub>2</sub> and H<sub>2</sub>S from biogas.  
8  
9  
10 4

#### 11 **Acknowledgments**

12  
13  
14 6 This research was supported by FAPESP, Brazil (process number 2009/15984-0 and  
15  
16 7 2013/17591-1), the CNPq (process number 158721/2012-8) and CONACyT México  
17  
18 8 (No. Reg: 237873). The financial support of Junta de Castilla y León (VA024U14 and  
19  
20 9 UIC 71) and the Latinoamerican Mobility Grants provided by Banco Santander are also  
21  
22 10 gratefully acknowledged.  
23  
24  
25  
26  
27  
28  
29  
30  
31  
32  
33  
34  
35  
36  
37  
38  
39  
40  
41  
42  
43  
44  
45  
46  
47  
48  
49  
50  
51  
52  
53  
54  
55  
56  
57  
58  
59  
60



1  
2  
3 **1 References**  
4

- 5  
6 1. Petersson A and Wellinger A, Biogas upgrading technologies – developments and  
7  
8 innovations. *IEA Bioenergy*, Task 37 (2009).  
9  
10  
11 2. Fernández M, Ramírez M, Pérez RM, Gómez JM and Cantero D, Hydrogen sulphide  
12  
13 removal from biogas by an anoxic biotrickling filter paced with Pall rings. *Chem Eng*  
14  
15 *J* **225**: 456-463 (2013).  
16  
17  
18 3. EurObserv'ER Website. Biogas Barometer N° 224 November 2014  
19  
20 <http://www.eurobserv-er.org/> [accessed 2 August 2015].  
21  
22  
23 4. Ramirez M, Gómez JM, Aroca G and Cantero D, Removal of hydrogen sulfide by  
24  
25 immobilized *Thiobacillus thiooparus* in a biotrickling filter packed with polyurethane  
26  
27 foam. *Biores Technol* **100**: 4989-4995 (2009).  
28  
29  
30 5. Fernández M, Ramírez M, Gómez JM and Cantero D, Biogas biodesulfurization in  
31  
32 an anoxic biotrickling filter packed with open-pore polyurethane foam. *J Hazard Mat*  
33  
34 **264**: 529-535 (2014).  
35  
36  
37 6. Tomàs M, Fortuny M, Lao C, Gabriel D, Lafuente F and Gamisans X, Technical and  
38  
39 economical study of a full-scale biotrickling filter for H<sub>2</sub>S removal from biogas.  
40  
41 *Water Pract Technol* **4**:2 (2009).  
42  
43  
44 7. Bahr M, Díaz I, Dominguez A, Gonzalez Sanchez A and Muñoz R, Microalgal-  
45  
46 biotechnology as a platform for an integral biogas upgrading and nutrient removal  
47  
48 from anaerobic effluents. *Environ Sci Technol* **48**: 573-571 (2014).  
49  
50  
51 8. González-Sánchez A, Revah S and Deshusses M, Alkaline Biofiltration of H<sub>2</sub>S  
52  
53 Odors. *Environ Sci Technol* **19**: 7398-7404 (2008).  
54  
55  
56  
57  
58  
59  
60

- 1  
2  
3 1 9. Cavalcanti PFF, Medeiros EJS, Silva JKM and Van Haandel A, Excess sludge  
4  
5 2 discharge frequency for UASB reactors. *Water Sci Technol* **40**: 211-219 (1999).  
6  
7  
8 3 10. American Public Health Association/American Water Works Association/Water  
9  
10 4 Environment Federation (APHA/AWWA/WEF). Standard Methods for the  
11  
12 5 Examination of Water and Wastewater. 21st edition, American Public Health  
13  
14 6 Association/American Water Works Association/Water Environment Federation,  
15  
16 7 Washington DC, USA (2005).  
17  
18  
19 8 11. Montebello AM, Fernández M, Almenglo F, Ramírez M, Cantero D, Baeza M  
20  
21 9 and Gabriel D, Simultaneous methylmercaptan and hydrogen sulfide removal in the  
22  
23 10 desulfurization of biogas in aerobic and anoxic biotrickling filters. *Chem Eng J*  
24  
25 11 **200–202**: 237–246 (2012).  
26  
27  
28 12 12. Wang A-J, Du D-Z, Ren N-Q, Van Groenestijn JW, An innovative process of  
29  
30 13 simultaneous desulfurization and denitrification by *Thiobacillus denitrificans*. *J*  
31  
32 14 *Environ Sci Heal A* **40**: 1939-1949 (2005).  
33  
34  
35 15 13. Janssen AJH, Ma SC, Lens P and Lettinga G, Performance of a sulfide-oxidizing  
36  
37 16 expanded-bed reactor supplied with dissolved oxygen. *Biotechnol Bioeng* **53**: 32-40  
38  
39 17 (1997).  
40  
41  
42 18 14. Soreanu G, Béland M, Falletta P, Edmonson K and Seto P, Laboratory pilot  
43  
44 19 scale study for H<sub>2</sub>S removal from biogas in an anoxic biotrickling filter. *Water Sci*  
45  
46 20 *Technol* **57**: 201-207 (2008a).  
47  
48  
49 21 15. Soreanu G, Béland M, Falletta P, Edmonson K and Seto P, Investigation on the  
50  
51 22 use of nitrified wastewater for the steady-state operation of a biotrickling filter for  
52  
53 23 the removal of hydrogen sulphide in biogas. *J Environ Eng Sci* **7**: 543-552 (2008b).  
54  
55  
56  
57  
58  
59  
60

- 1  
2  
3 16. Estrada JM, Lebrero R, Quijano G, Pérez R, Figueroa-González I, García-Encina  
4  
5 PA and Muñoz R, Methane abatement in a gas-recycling biotrickling filter:  
6  
7 Evaluating innovative operational strategies to overcome mass transfer limitations.  
8  
9 *Chem Eng J* **253**: 385-393 (2014).  
10  
11  
12 17. Kao C-Y, Chiu S-Y, Huang T-T, Dai L, Hsu L-K and Lin C-S, Ability of a  
13  
14 mutant strain of the microalga *Chlorella* sp. to capture carbon dioxide for biogas  
15  
16 upgrading. *App Energ* **93**: 176-183 (2012).  
17  
18  
19 18. Wang Z, Zhao Y, Ge Z, Zhang H, Sun S, Selection of microalgae for  
20  
21 simultaneous biogas upgrading and biogas slurry nutrient reduction under various  
22  
23 photoperiods. *J Chem Technol Biot Online first* (2015)  
24  
25  
26 19. Cheah WY, Show PL, Chang J-S, Ling TC and Juan JC, Biosequestration of  
27  
28 atmospheric CO<sub>2</sub> and flue gas-containing CO<sub>2</sub> by microalgae. *Bioresour*  
29  
30 *Technol* **184**: 190-201 (2015).  
31  
32  
33 20. Mann G, Schelgel M, Schumann R and Sakalauskas A, Biogas conditioning with  
34  
35 microalgae. *Agron Res* **7**: 33-38 (2009).  
36  
37  
38 21. Serejo M, Posadas E, Boncz M, Blanco S, García-Encina PA and Muñoz R,  
39  
40 Influence of biogas flow rate on biomass composition during the optimization of  
41  
42 biogas upgrading in microalgal-bacterial processes. *Environ Sci Technol* **49**: 3228-  
43  
44 3236 (2015).  
45  
46  
47  
48  
49  
50  
51  
52  
53  
54  
55  
56  
57  
58  
59  
60

1  
2  
3 **1 Figure captions**

4  
5 **2 Figure 1.** Schematic diagram of the biotrickling filter (A) and the photobioreactor (B)  
6  
7 for biogas upgrading.  
8

9  
10  
11 **5 Figure 2.** Time course of (A) the inlet (■) and outlet (□) H<sub>2</sub>S concentrations, and EBRT  
12  
13 (×) of the biogas upgraded in the BTF; and (B) CH<sub>4</sub> (◆), CO<sub>2</sub> (◇) and H<sub>2</sub>S (□) removal  
14  
15 efficiencies in the BTF. The grey area represents the shutdown period and the vertical  
16  
17 dashed line the beginning of digestate supplementation.  
18  
19

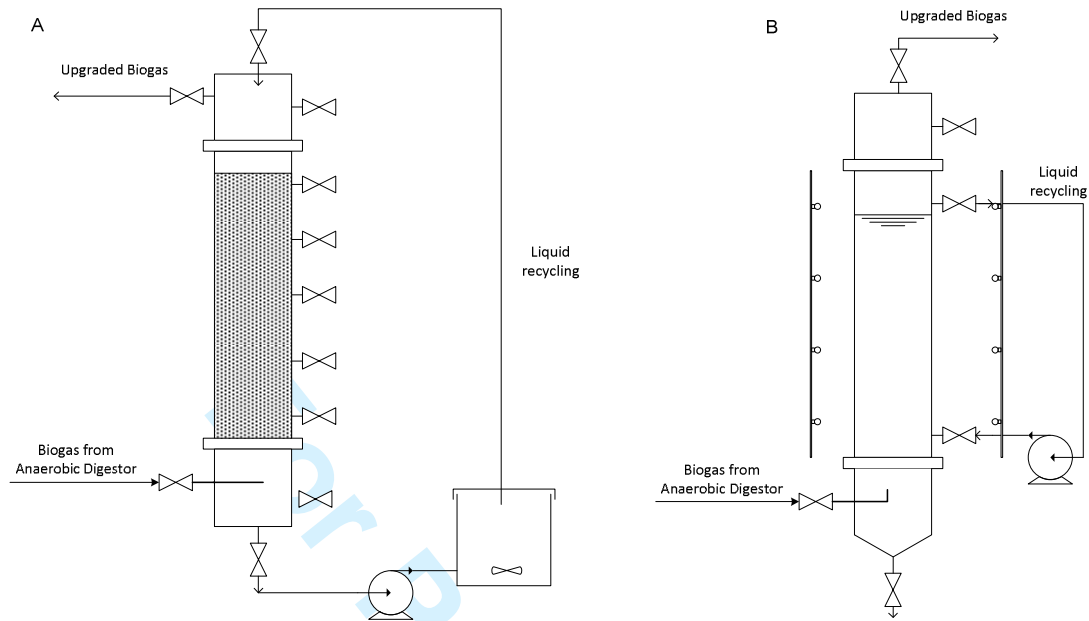
20  
21  
22 **10 Figure 3.** Time course of (A) sulfate (□), nitrate (●), nitrite (○) and sulfur (×)  
23  
24 concentrations in the BTF recycling media; and (B) Sulfur inlet load (◆) and nitrate  
25  
26 consumption rate (◇). The grey area represents the shutdown period and the vertical  
27  
28 dashed line the beginning of digestate supplementation.  
29  
30  
31

32  
33  
34 **15 Figure 4.** Bacterial similarity dendogram (UPGMA clustering) and DGGE profile of  
35  
36 the bacterial communities present in the inoculum, digestate and the samples from the  
37  
38 carrier at the top (R1), medium (R2) and bottom (R3) of the BTF.  
39  
40  
41

42  
43 **19 Figure 5.** Time course of (A) the inlet (■) and outlet (□) H<sub>2</sub>S concentrations, and EBRT  
44  
45 (×) of the biogas upgraded in the FBR; and (B) CH<sub>4</sub> (◆), CO<sub>2</sub> (◇) and H<sub>2</sub>S (○) removal  
46  
47 efficiencies in the FBR.  
48

49  
50  
51 **23 Figure 6.** Time course of sulfate (□) and sulfur (×) concentration in the PBR cultivation  
52  
53 broth, and sulfur inlet load (◆).  
54  
55

56  
57  
58  
59  
60

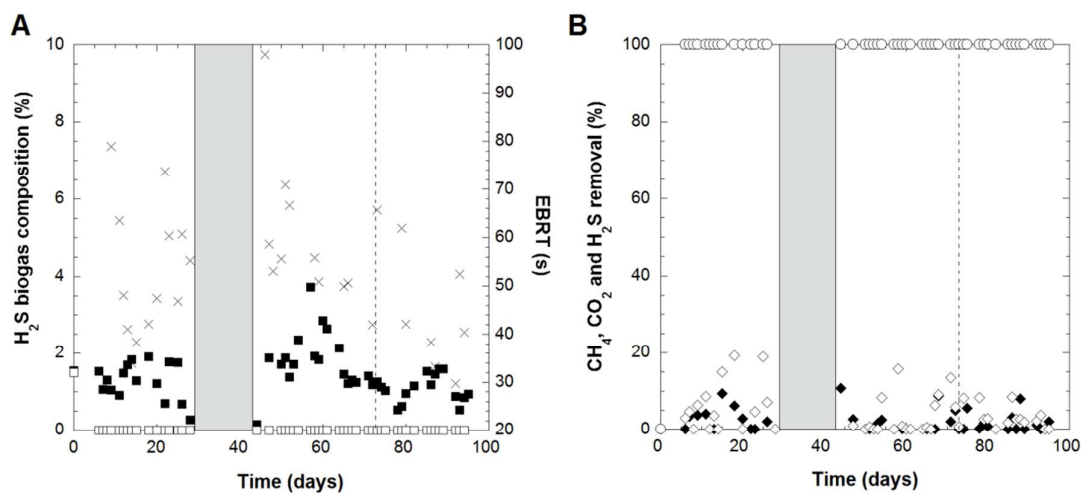
1 **Figure 1.**

2

3 **Figure 1.** Schematic diagram of the biotrickling filter (A) and the photobioreactor (B)

4 for biogas upgrading.

5

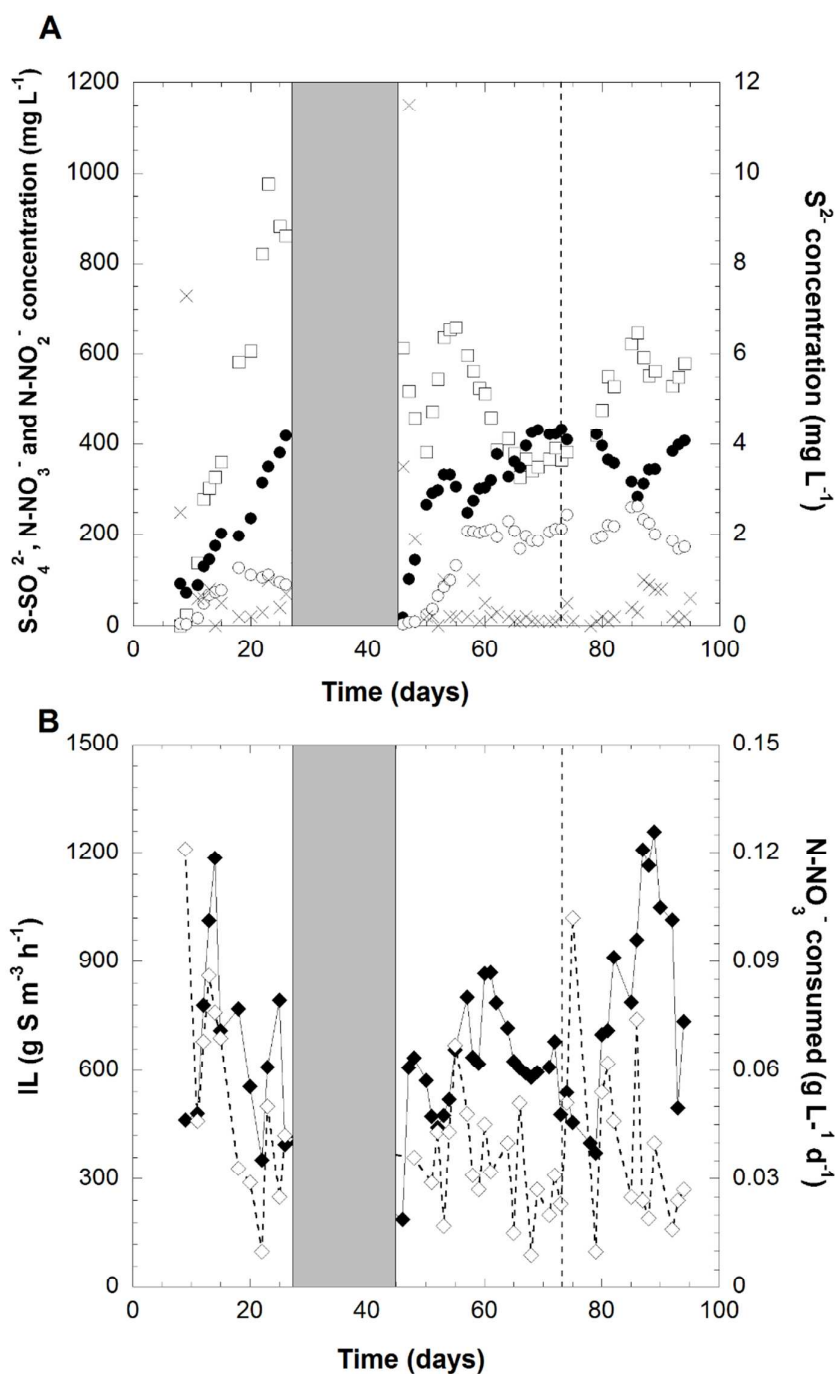
1 **Figure 2.**

2

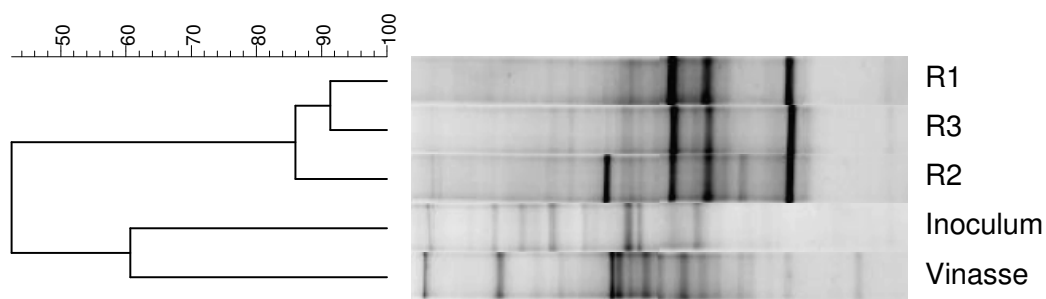
3 **Figure 2.** Time course of (A) the inlet (■) and outlet (□) H<sub>2</sub>S concentrations, and EBRT  
4 (×) of the biogas upgraded in the BTF; and (B) CH<sub>4</sub> (◆), CO<sub>2</sub> (◇) and H<sub>2</sub>S (○) removal  
5 efficiencies in the BTF. The grey area represents the shutdown period and the vertical  
6 dashed line the beginning of digestate supplementation.

7

1 Figure 3.

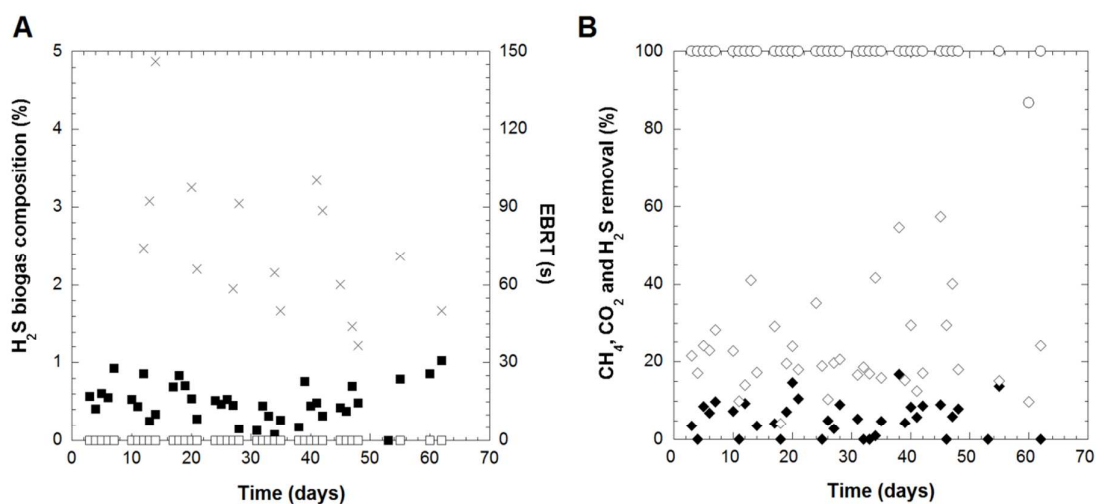


2  
3 **Figure 3.** Time course of (A) sulfate (□), nitrate (●), nitrite (○) and sulfur (×)  
4 concentrations in the BTF recycling media; and (B) Sulfur inlet load (◆) and nitrate  
5 consumption rate (◇). The grey area represents the shutdown period and the vertical  
6 dashed line the beginning of digestate supplementation.

1 **Figure 4.**

2  
3 **Figure 4.** Bacterial similarity dendrogram (UPGMA clustering) and DGGE profile of  
4 the bacterial communities present in the inoculum, digestate and the samples from the  
5 carrier at the top (R1), medium (R2) and bottom (R3) of the BTF.  
6  
7  
8  
9  
10

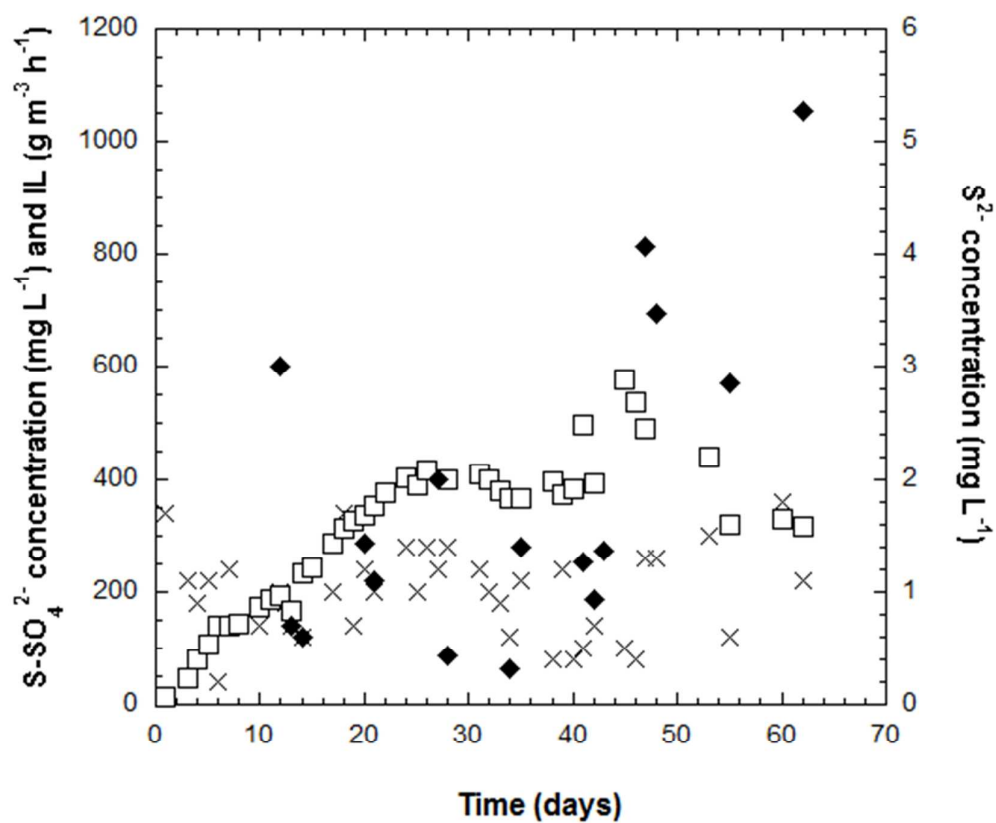


1 **Figure 5.**

2

3 **Figure 5.** Time course of (A) the inlet (■) and outlet (□) H<sub>2</sub>S concentrations, and EBRT  
 4 (×) of the biogas upgraded in the FBR; and (B) CH<sub>4</sub> (◆), CO<sub>2</sub> (◇) and H<sub>2</sub>S (○) removal  
 5 efficiencies in the FBR  
 6  
 7  
 8  
 9  
 10  
 11  
 12  
 13  
 14  
 15  
 16  
 17  
 18  
 19

1 Figure 6.



2

3 **Figure 6.** Time course of sulfate (□) and sulfur (×) concentration in the PBR cultivation  
4 broth, and sulfur inlet load (◆)

5

6

7